Design and Optimization of a MEMS Electret-Based Capacitive Energy Scavenger

Fabio Peano and Tiziana Tambosso, *Senior Member, IEEE*

***Abstract*—In this paper, a method for the design and optimization of an electret-based vibration-to-electric microconverter is presented, using a nonlinear dynamical model of the device. The dynamics of the converter is analyzed in detail, showing the importance of properly accounting for the nonlinearity in the optimization process. A procedure to determine a set of optimization parameters is finally presented. [1323]**

***Index Terms*—Capacity converters, electret, energy harvesting, microelectromechanical systems (MEMS).**

I. Introduction

In the last years, much interest has been attracted by microgenerators capable of extracting power from ambient vibrations, a process known as energy scavenging. Several techniques to perform electromechanical energy conversion have been proposed, and a good review is presented in [1]. Basically, we find three classes of electromechanical converters: *inductive* [2]–[4], *piezoelectric* [5]–[7] and *capacitive* [8]–[11]. The last class offers a good capability of miniaturization and on-chip integration, but usually needs a voltage bias for the conversion process to occur [1], [8], [9].

In this work, we focus on a new method of capacitive conversion, proposed by Sterken *et al.* [10], [11], which does not require the external voltage bias. The basic schematic of the converter, shown in Fig. 1, uses an electret [12], [13] sandwiched between two electrodes, one fixed (B, the substrate) and the other (A, the proof mass) actuated by ambient vibrations. Vibrations cause a flow of charge between the fixed electrode B and the two variable capacitors C_1 and C_2.

We can schematize the process by means of the equivalent circuit of Fig. 2, which will be used in Section II to analyze the converter dynamics. Despite it looks very simple, the equivalent circuit is not easy to treat in closed form, because the voltage on the capacitors C_1 and C_2 are nonlinear in the mass displacement. Thus, an explicit expression for the extracted output power is difficult to find, and we have to resort to numerical solutions.

In the optimization process, we are faced with a time-consuming numerical integration, depending on the number of free parameters. Thus, the critical step is the choice of a minimum set of optimization parameters, as discussed in Section III. Finally, to validate the proposed method, we present a comparison of our results with those of the small signal (linearized) model, based on the case analyzed by Sterken *et al.* [10], [11].

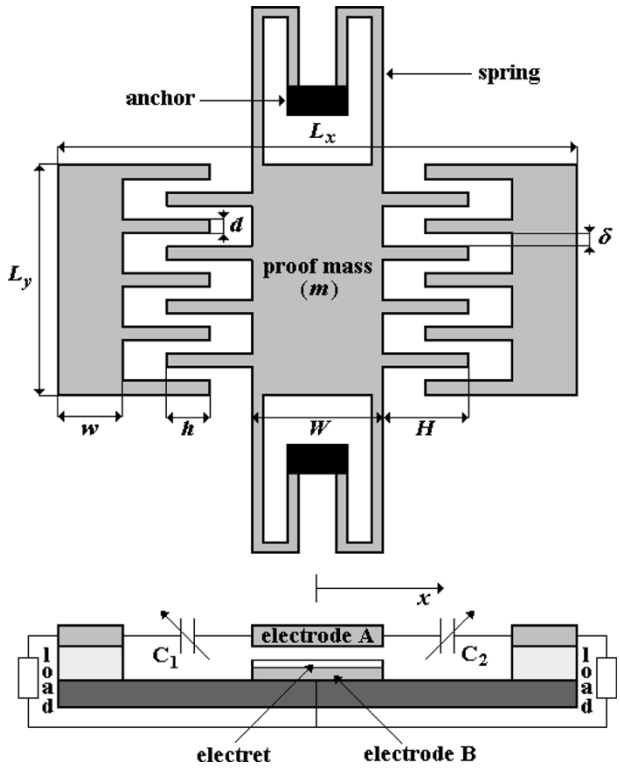

Fig. 1. The electret-based capacitive converter: reference structure (top view) and charge exchange through C_1 and C_2 (side view).

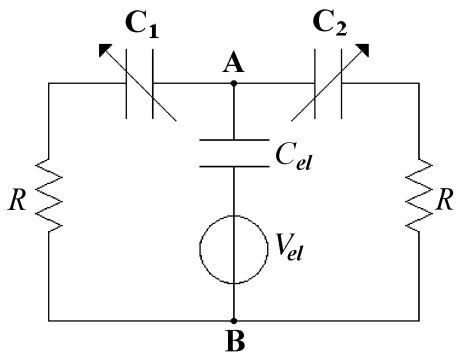

Fig. 2. Equivalent electric circuit of the converter.

II. Dynamical Model of the Converter

In order to work out a dynamical model of the converter, we start writing the voltage $V = Q/C$ at the electrodes, and the magnitude of the electrostatic force $F = d(qV/2)/dx$ of a

Manuscript received May 5, 2004; revised October 8, 2004. Subject Editor G. B. Hocker.

F. Peano is with Politecnico di Torino, Department of Energetic, Turin, Italy.

T. Tambosso is with Telecom Italia Lab, 10148 Turin, Italy (e-mail: tiziana.tambosso@telecomitalia.it).

Digital Object Identifier 10.1109/JMEMS.2005.844803

single comb-like variable capacitor of capacitance C, as functions of the charge q at the electrodes and of the displacement x off the initial overlap h

$$\begin{cases} V(q,x) = \frac{q\delta}{2N\varepsilon_0 b(h-x)} \\ F(q,x) = \frac{q^2\delta}{4N\varepsilon_0 b(h-x)^2} \end{cases} \tag{1}$$

where ε_0 is the dielectric constant of vacuum, N the number of fingers, b the height of the fingers, h and δ the initial overlap and the gap between movable and fixed fingers (see Fig. 1), respectively. For a symmetric structure with two identical capacitors, we have

$$\begin{cases} F_1(q_1,x) = F(q_1,x) \\ V_1(q_2,x) = V(q_1,x) \\ F_2(q_1,x) = F(q_2,-x) \\ V_2(q_2,x) = V(q_2,-x) \end{cases}. \tag{2}$$

Using (1) and (2), we can write the equations governing the dynamic of the converter in the following form:

$$\begin{cases} R\frac{dq_1}{dt} = -V_1(q_1,x) - \frac{q_1+q_2}{C_{el}} + V_{el} \\ R\frac{dq_2}{dt} = -V_2(q_2,x) - \frac{q_1+q_2}{C_{el}} + V_{el} \\ m\frac{d^2x}{dt^2} = F_2(q_2,x) - F_1(q_1,x) - kx - B\frac{dx}{dt} - ma(t) \end{cases}. \tag{3}$$

Here, the third equation is the law of dynamics, m, k, B and $a(t)$ being, respectively, the mass of the mechanical resonator, the mechanical stiffness, the damping coefficient and the acceleration caused on the device by the external vibration source, which, from now on, will be assumed to be periodic with period T. The first two equations describe the electret placed between the electrodes A and B, through a model of a capacitance C_{el} and a constant voltage source V_{el} [11], [12], R being the load resistance (Fig. 2).

For the purpose of generality, we rewrite (3) using normalized variables, by setting

$$\hat{t} = t\omega_1, \quad \hat{q}_1 = \frac{q_1}{q_0}, \quad \hat{q}_2 = \frac{q_2}{q_0}, \quad \hat{x} = \frac{x}{h}, \tag{4}$$

where $\omega_1/2\pi$ is the mechanical resonance frequency of the device, and q_0 is the initial charge on each variable capacitor. The charge q_0 is given by $q_0 = C_0V_0$, C_0 and V_0 being the capacitance and quiescent voltage for each variable capacitor, written as

$$C_0 = \frac{2N\varepsilon_0 bh}{\delta}, \quad V_0 = \frac{C_{el}}{2C_0 + C_{el}}V_{el}. \tag{5}$$

Using the above definitions, (3) in normalized form become

$$\begin{cases} \frac{d\hat{q}_1}{d\hat{t}} = -\hat{\omega}_2\frac{\hat{q}_1}{1-\hat{x}} - \hat{\omega}_{el}(\hat{q}_1+\hat{q}_2) + \hat{I}_{el} \\ \frac{d\hat{q}_2}{d\hat{t}} = -\hat{\omega}_2\frac{\hat{q}_2}{1+\hat{x}} - \hat{\omega}_{el}(\hat{q}_1+\hat{q}_2) + \hat{I}_{el} \\ \frac{d^2\hat{x}}{d\hat{t}^2} = -\frac{\eta}{2}\left[\frac{\hat{q}_1}{1-\hat{x}}\right]^2 + \frac{\eta}{2}\left[\frac{\hat{q}_2}{1+\hat{x}}\right]^2 - \hat{x} - 2\zeta\frac{d\hat{x}}{d\hat{t}} - \hat{a}(\hat{t}) \end{cases} \tag{6}$$

where we have introduced the normalized quantities

$$\hat{\omega}_2 = \frac{1}{RC_0\omega_1}, \quad \hat{\omega}_{el} = \frac{1}{RC_{el}\omega_1}, \quad \hat{I}_{\rm el} = \frac{V_{el}}{RC_0V_0\omega_1}, \quad \eta = \frac{C_0V_0^2}{mh^2\omega_1^2}, \quad \zeta = \frac{B}{2m\omega_1}, \quad \hat{a}(\hat{t}) = \frac{a(t)}{h\omega_1^2}. \tag{7}$$

Once (6) is solved, we can calculate the output power $P_{\rm out}$ supplied by the generator as the time average of

$$P(t) = C_0V_0^2\omega_1\hat{P}(\hat{t}) \tag{8}$$

being

$$\hat{P}(\hat{t}) = \frac{1}{\hat{\omega}_2}\left[\left(\frac{d\hat{q}_1}{d\hat{t}}\right)^2 + \left(\frac{d\hat{q}_2}{d\hat{t}}\right)^2\right] \tag{9}$$

the normalized instantaneous power. As we can see, $\hat{P}(\hat{t})$ depends only on the normalized parameters $\hat{\omega}_2, \hat{\omega}_{el}, \eta, \zeta$, of which $\hat{\omega}_2$ describes the load impedance and η is about the relative strength of the electrostatic forces with respect to the inertial forces.

An explicit expression for $P_{\rm out}$ can be derived for the small signal regime, i.e., for small oscillations and small charge variations

$$\left(\left|\hat{x}(\hat{t})\right| \ll 1\right) \quad \text{and} \quad \left(\left|\hat{q}_{1,2}(\hat{t}) - 1\right| \ll 1\right). \tag{10}$$

Indeed, by linearizing (6) about the equilibrium working point in absence of excitation ($\hat{q}_1(\hat{t}) = 1, \hat{q}_2(\hat{t}) = 1, \hat{x}(\hat{t}) = 0$), one obtains the following linear set of equations:

$$\begin{cases} \frac{d\hat{Q}}{d\hat{t}} = -(\hat{\omega}_2 + 2\hat{\omega}_{el})\hat{Q} \\ \frac{d\hat{q}}{d\hat{t}} = -\hat{\omega}_2\hat{q} + \hat{\omega}_2\hat{x} \\ \frac{d^2\hat{x}}{d\hat{t}^2} = -2\eta\hat{q} - (1+2\eta)\hat{x} - 2\zeta\frac{d\hat{x}}{d\hat{t}} - \hat{a}(\hat{t}) \end{cases} \tag{11}$$

being

$$\begin{cases} \hat{Q} = \delta\hat{q}_1 + \delta\hat{q}_2 \\ \hat{q} = \frac{\delta\hat{q}_1 - \delta\hat{q}_2}{2} \end{cases} \tag{12}$$

with $\delta\hat{q}_{1,2} = \hat{q}_{1,2} - 1$. As we can see, the first equation in (11) is independent from the others and its solution is just the exponential charge/discharge transient for the electret capacitance C_{el}, which means that, in asymptotic regime, $\hat{Q}(\hat{t}) = 0$ and no current passes through C_{el}. Equations (11) are a set of two equations in the variables $\hat{q}$ and $\hat{x}$; accordingly, for a sinusoidal mechanical input $\hat{a}(\hat{t}) = -\hat{\rm A}\sin(\hat{\omega}\hat{t})$, the output power is found analytically as

$$P_{\rm out} = C_0V_0^2\omega_1\hat{P}_{\rm out} \tag{13}$$

where

$$\hat{P}_{\text{out}} = \frac{\hat{\omega}_2 \hat{\omega}^2 \hat{\text{A}}^2}{\left\{ \left[\hat{\omega}_2 - (\hat{\omega}_2 + 2\zeta)\hat{\omega}^2 \right]^2 + \hat{\omega}_2 \left[1 + 2\eta - \hat{\omega}^2 + 2\zeta\hat{\omega}_2 \right]^2 \right\}} \tag{14}$$

Though valid only in the small-oscillation regime, (14) provides a straightforward and useful estimate of the output power for a specific application. However, the linear model cannot be used in general and there is no reason for the optimal parameters to correspond to a small oscillations regime. Therefore, in order to set up a general design-and-optimization procedure, as carried out in next section, we must resort to the nonlinear model (6).

III. Design and Optimization of the Device

A. Preliminary Considerations

Before starting the design and optimization, we should check that the electret-based capacitive converter be a suitable solution for the intended application. This is easily done by considering the normalized output power, $\hat{P}_{\text{out}}$, expressed as

$$\hat{P}_{\text{out}} = \hat{P}_{\text{in}} - \hat{P}_{\text{loss}} \tag{15}$$

where, as it is shown in Appendix A, $\hat{P}_{\text{in}}$ is the average value of $\hat{P}_{\text{mech}}$, the mechanical power absorbed by the converter and $\hat{P}_{\text{loss}}$ is the average value of $\hat{P}_{\text{damp}}$, the power loss due to damping, and these quantities are given respectively by

$$\hat{P}_{\text{mech}} = -\frac{\hat{a}(\hat{t})}{\eta}\frac{d\hat{x}}{d\hat{t}} \quad \text{and} \quad \hat{P}_{\text{damp}} = \frac{2\zeta}{\eta}\left(\frac{d\hat{x}}{d\hat{t}}\right)^2. \tag{16}$$

If the vibration exciting the generator has a power spectrum with a peak frequency, $\omega/2\pi$, we can assume the driving term $a(t)$ in (3) as a simple sinusoid

$$a(t) = -A\sin(\omega t) \tag{17}$$

where A is the amplitude of the acceleration. Then, as long as the loss term is neglected, we can write

$$P_{\text{out}} = -\frac{m\omega}{2\pi}\int_t^{t+T} a(t)\frac{dx}{dt}dt = \frac{m\omega}{2\pi}\int_t^{t+T} x\frac{da(t)}{dt}dt \tag{18}$$

where $T = 2\pi/\omega$ is the oscillation period, and, if also $x(t)$ can be assumed sinusoidal, i.e.

$$x(t) \cong X\sin(\omega t + \varphi) \tag{19}$$

an estimate for P_{out}, in the most favorable case $\varphi = -\pi/2$ (with respect to the driving inertial force, $-a(t) = A\sin(\omega t)$), follows as

$$P_{\text{out}} \cong \frac{1}{2}m\omega AX = \frac{1}{2}m\omega^3 YX \tag{20}$$

being Y the oscillation amplitude of the vibration source. Now, by taking into account the constraints of fabrication, reasonable values for m and X can be chosen, and P_{out} can be estimated. Depending on both the output power required for the intended application and the maximum volume allowed, (20) can be used to analyze the applicability of this kind of energy scavenger with a given source of vibration.

B. Design and Optimization of Parameters

According to the model described in Section II, and assuming a sinusoidal vibration source, the output power depends on the quantities C_0, C_{el}, V_{el}, R, m, h, ω_1, B, A and ω. The last two depend on the mechanical source available, whereas R and ω_1 can be assumed as free parameters; the remaining quantities depend on the geometrical structure of the device. We can get a simplification by assuming the volume to be the maximum allowed by the application, that is, maximizing L_x, L_y and b. The mass m can then be written as

$$m = \rho b(L_y W + 2NHd) \tag{21}$$

ρ being the material density (for Si, $\rho = 2330\ \text{Kg/m}^3$). We have also

$$W = L_x - 2(2H + w - h), \quad N \cong \frac{L_y}{2(d+\delta)} \tag{22}$$

The mass m depends on five parameters, H, w, h, d, and δ, among which one or more free parameters can be chosen. In this work, we take h as an optimization parameter and the aspect ratios b/d, b/δ, h/H and h/w are set to a fixed value as follows:

$$\begin{cases} r_1 = \frac{b}{\delta} = 25 \\ r_2 = \frac{b}{d} = 25 \\ r_3 = \frac{h}{H} = 0.5 \\ r_4 = \frac{h}{w} = 0.5 \end{cases}. \tag{23}$$

According to (22) and (23) one can write

$$m = m(h) = \rho b L_y(L_x - 9h) \tag{24}$$

and

$$C_0 = C_0(h) = r_2^2\frac{\varepsilon_0 L_y h}{2b} \tag{25}$$

where h will satisfy the constraint

$$0 < h < \frac{L_x}{14}. \tag{26}$$

For simplicity, we now assume a fixed value for the remaining parameters, V_{el}, C_{el}, and B too, despite their eventual dependence on the geometrical parameters (e.g. on h) could improve optimization further. Also, we assume a fixed value for the gap between electrode A and the electret, which should be as low as possible, in order to maximize C_{el} and, consequently, V_0.

Under this assumption, by computing the normalized quantities given by (7) by means of (24) and (25) one can formally write P_{out} as a function of the three parameters ω_1, R and h:

$$P_{\text{out}}(\omega_1, h, R) = C_0(h)V_0^2(h)\frac{\omega}{2\pi}\int_{\hat{t}}^{\hat{t}+\hat{T}} \hat{P}(\omega_1, R, h, \hat{t})d\hat{t}, \tag{27}$$

being $\hat{T} = 2\pi/\hat{\omega}$ the normalized oscillation period. Once the ranges of variation for ω_1, R and h are provided, the design can be optimized by looking for the combination that maximizes P_{out}. This procedure is general and applicable to a wide

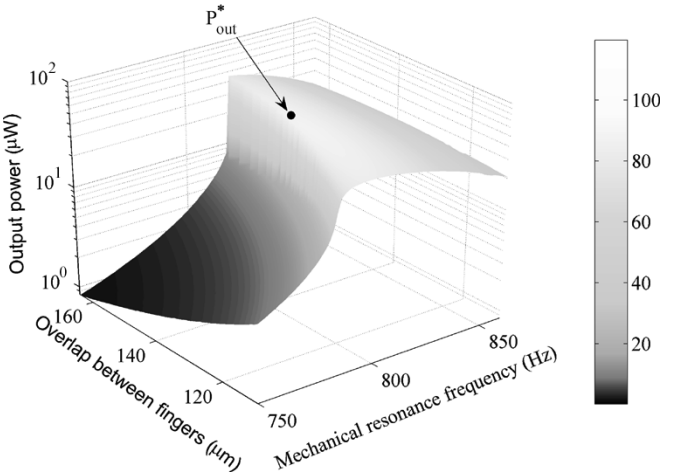

Fig. 3. Output power as a function of the optimization parameters h (the quiescent finger overlap) and ω_1 (the mechanical resonance frequency) for the optimal load value, $R = R^* = 70\ \mathrm{M\Omega}$.

range of cases and working conditions, depending on the particular application. Also, the design-and-optimization scheme here proposed can be easily modified, if needed; for instance, one could employ a different set of free parameters, or different geometrical aspect ratios (as long as geometrical quantities are included among the optimization parameters, all these choices greatly affect the final design of the device). In the next section, we present an example of application.

C. An Example of Design-and-Optimization

The example reported here is based on the case considered by Sterken *et al.* in [10], [11]. According to (7), (24), and (25) the system is defined by the following set of fixed parameters:

$$\begin{array}{|l|l|}\hline V_{el} = 150\ \mathrm{V} & C_{el} = 16.8\ \mathrm{pF} \\ \hline L_x = 2.3\ \mathrm{mm} & L_y = 5\ \mathrm{mm} \\ \hline b = 100\ \mu\mathrm{m} & \mathrm{B} = 25.5\ \mu\mathrm{Ns/m} \\ \hline \end{array} . \tag{28}$$

The vibration source of excitation [11] is a sinusoidal oscillation with amplitude $Y = 5\ \mu\mathrm{m}$ and frequency $\omega/2\pi = 911$ Hz, so that a sinusoidal driving term can be considered with

$$\begin{cases} \omega = 5724\ \mathrm{rad/s} \\ A = 163.8\ \mathrm{m/s^2} \end{cases} . \tag{29}$$

About the constraints on parameters, the following ranges of variation are assumed:

$$\begin{cases} 0.5\omega \le \omega_1 \le \omega \\ 0 \le h \le \frac{L_x}{14}(164\ \mu\mathrm{m}) \\ 10\ \mathrm{M\Omega} \le R \le 500\ \mathrm{M\Omega} \end{cases} . \tag{30}$$

The maximum of output power is now searched by solving (6) on a suitable 3-D grid in the space of parameters (this has been performed using the standard ODE solvers available in MATLAB. The use of a proper 3-D grid leads to computational times up to a week on a fast PC running MATLAB 6.1 for Windows. For the example here reported a $64 \times 64 \times 64$ grid in the (ω_1, R, h) space has been used. If one chose to use a higher number of free parameters, the computational effort would grow tremendously and the development of an ad hoc numerical technique would probably be required). Doing so, we find the optimal set of parameters (which we mark with an asterisk)

$$\begin{cases} \omega_1^* \cong 5080\ \mathrm{rad/s}(0.89\omega) \\ h^* \cong 140\ \mu\mathrm{m} \\ R^* \cong 70\ \mathrm{M\Omega} \end{cases} \tag{31}$$

and the corresponding output power $P^*_{\mathrm{out}} = P_{out}(\omega_1^*, h^*, R^*) = 50\ \mu\mathrm{W}$. Fig. 3 shows a plot of $P_{\mathrm{out}}(\omega_1, h, R = R^*)$. Figs. 4 to 7 describe quantities relative to the asymptotic solution of (6) in the case of optimal configuration of free parameters, $(\omega_1, h, R) = (\omega_1^*, h^*, R^*)$. In Fig. 4, the mass displacement $(\hat{x})$ and the external oscillation $(\hat{y})$ are plotted on a period, being

$$\hat{y}(\hat{t}) = \hat{Y}\sin(\hat{\omega}\hat{t}) \tag{32}$$

where $\hat{Y} = Y/h$ is the normalized oscillation amplitude. The oscillation $\hat{x}$ is nearly sinusoidal with amplitude $\hat{X} = X/h \cong 0.7$, meaning that the first condition of (10) is violated and the regime is highly non linear, as clearly revealed by the waveforms of $\hat{q}_1$, $\hat{q}_2$, $d\hat{q}_1/d\hat{t}$ and $d\hat{q}_2/d\hat{t}$ reported in Figs. 5 and 6. Finally,

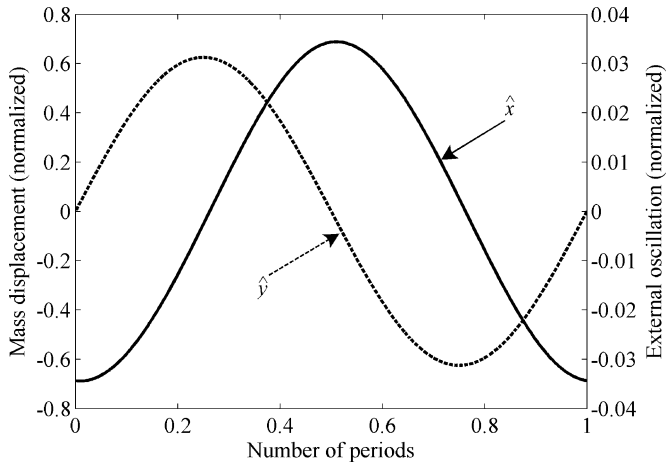

Fig. 4. Proof mass displacement $(\hat{x})$ during a complete oscillation of the external vibration excitation $(\hat{y})$, in the asymptotic regime.

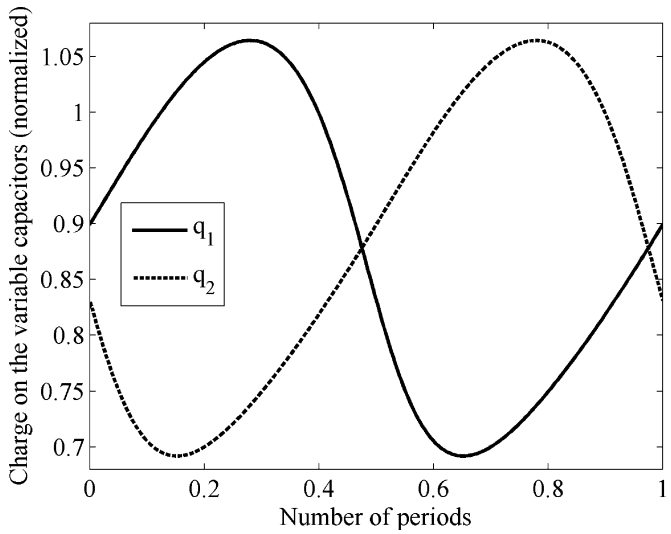

Fig. 5. Waveform of the charge on each variable capacitor on a period of excitation.

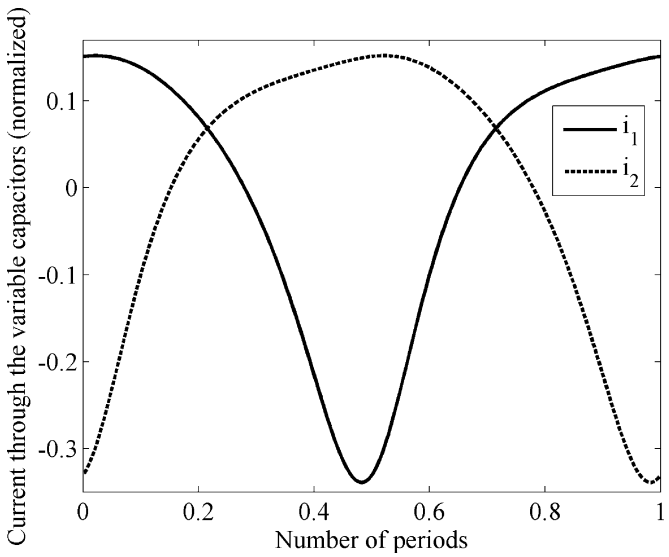

Fig. 6. Waveform of current in each variable capacitor on a period of excitation.

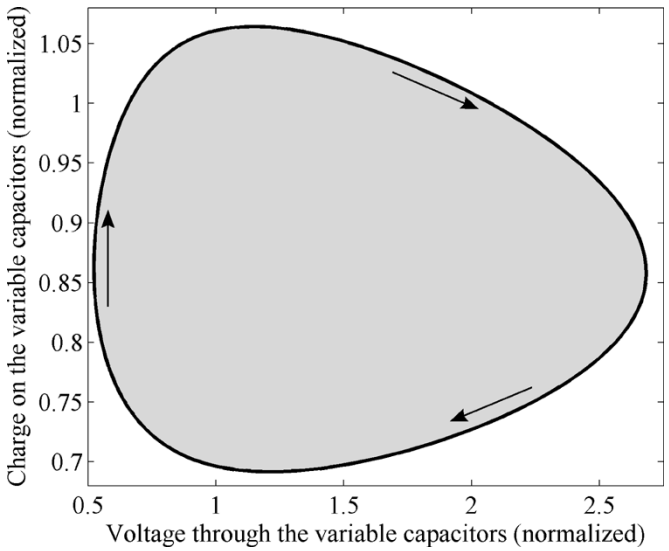

Fig. 7. Charge-voltage conversion cycle of the device. The loop area is half the converted energy per cycle.

Fig. 7 is a plot of the conversion cycle, that is, the cycle described in the voltage-charge plane during an oscillation period [8]. For symmetry reasons, the cycle is equal on both variable capacitors and its area is equal to half the total energy converted per cycle.

The example reported above is a typical case where good combinations of free parameters correspond to highly nonlinear regimes, meaning that they could not be found in the framework of the linear model (11). In fact, by inserting the optimized data in (13), (14), we find $P_{\rm out} = 6\ \mu$W, a value much lower than that obtained with the nonlinear model. On the other hand, if we repeated the same optimization procedure discussed above evaluating $P_{\rm out}$ through (13), (14), rather than solving (6), we would find

$$\begin{cases} \omega_1^* \cong 5179\ \text{rad/s}(0.90\omega) \\ h^* \cong 98\ \mu\text{m} \\ R^* \cong 500\ \text{M}\Omega \end{cases} \tag{33}$$

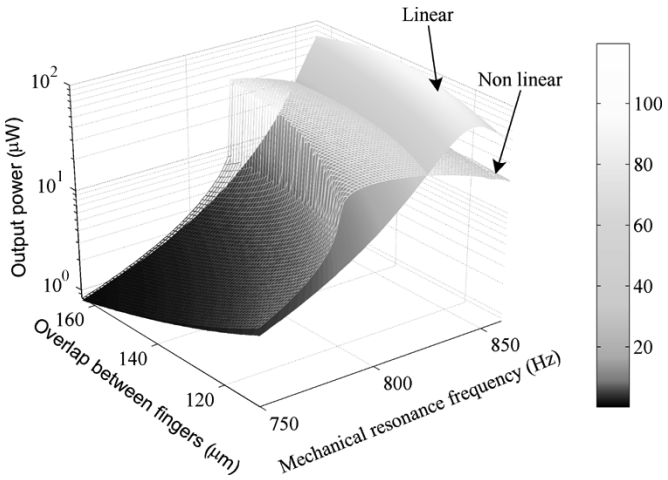

Fig. 8. Comparison of output powers $P_{\rm out}(h, \omega_1, R = R^* = 70\ \text{M}\Omega)$ obtained using the linear model and the nonlinear one.

as optimal set of parameters, and $P_{\rm out}^* = 283\ \mu$W as maximum output power. This last value is completely wrong and the parameters (33) are far from the real optimal parameters (31). For the combination of parameters (33), the real value of the output power (obtained from the solution of (6)) is $P_{\rm out} = 5.8\ \mu$W. Again, the corresponding regime is strongly nonlinear, involving mass displacements as high as $|\hat{x}| \cong 0.6$: such dynamic regimes cannot be described appropriately with the linear theory, due to the strong effects of the nonlinearity in the electromechanical coupling terms in (6). In general, very large differences between models (6) and (11) are likely to arise whenever one makes an improper use of the linear model, i.e., whenever conditions (10) are violated, which is the case of both set of parameters (31) (the correct optimal set) and (33) (the incorrect optimal set). This is well illustrated in Fig. 8 where a plot of $P_{\rm out}(h, \omega_1, R = R^* = 70\ \text{M}\Omega)$ obtained using the linear model is reported, compared with the plot of Fig. 3. For low values of $P_{\rm out}$, the two plots are similar (i.e., the regime is almost linear), but in the region of interest (high values of $P_{\rm out}$) they are completely different, because of the improper use of the linear approximation in these conditions.

IV. Conclusion

We developed a method for the design and optimization of an electret-based capacitive converter, based on the nonlinear dynamical model (6). As the procedure requires a numerical solution of the governing equations for each combination of free parameters, we adopted a series of constraints (technology driven) on the design of the device in order to reduce the number of free parameters, and, consequently, the required computational time. An example of application is reported showing that the nonlinear behavior of the converter is crucial in the optimization process and has to be taken into account to get correct results. From a 911 Hz vibration source with an oscillation amplitude of 5 μm, we can extract a maximum output power of 50 μW, obtained using the optimal combination of dimensional parameters calculated with the nonlinear model. Such a working point could not be found applying the small-signal, linear theory. Indeed, a much lower power (i.e., 5.8 μW) will be extracted from

a device whose design parameters are optimized with the linear model.

APPENDIX

Let us consider the energy balance for the converter, and rewrite (6) in terms of normalized power

$$\begin{cases} \frac{1}{\hat{\omega}_2}\left(\frac{d\hat{q}_1}{d\hat{t}}\right)^2 = \left[-\frac{\hat{q}_1}{1-\hat{x}} - \frac{\hat{\omega}_{el}}{\hat{\omega}_2}(\hat{q}_1+\hat{q}_2)+\hat{V}_{el}\right]\frac{d\hat{q}_1}{d\hat{t}} \\ \frac{1}{\hat{\omega}_2}\left(\frac{d\hat{q}_2}{d\hat{t}}\right)^2 = \left[-\frac{\hat{q}_2}{1+\hat{x}} - \frac{\hat{\omega}_{el}}{\hat{\omega}_2}(\hat{q}_1+\hat{q}_2)+\hat{V}_{el}\right]\frac{d\hat{q}_2}{d\hat{t}} \\ \frac{1}{\eta}\left(\hat{v}\frac{d\hat{v}}{d\hat{t}}\right) = \left[-\frac{1}{2}\left[\frac{\hat{q}_1}{1-\hat{x}}\right]^2+\frac{1}{2}\left[\frac{\hat{q}_2}{1+\hat{x}}\right]^2-\frac{\hat{x}}{\eta}-2\frac{\zeta}{\eta}\hat{v}-\frac{\hat{a}(\hat{t})}{\eta}\right]\hat{v} \end{cases} \tag{34}$$

where $\hat{v} = d\hat{x}/d\hat{t}$ and $\hat{V}_{el} = V_{el}/V_0 = \hat{I}_{el}/\hat{\omega}_2$. Now, one can eliminate the electro-mechanical coupling terms, using the energy balance equations for the two variable capacitors

$$\begin{cases} \frac{d}{d\hat{t}}\left[\frac{1}{2}\frac{\hat{q}_1^2}{1-\hat{x}}\right] = \frac{\hat{q}_1}{1-\hat{x}}\frac{d\hat{q}_1}{d\hat{t}} + \frac{1}{2}\left[\frac{\hat{q}_1}{1-\hat{x}}\right]^2\hat{v} \\ \frac{d}{d\hat{t}}\left[\frac{1}{2}\frac{\hat{q}_2^2}{1+\hat{x}}\right] = \frac{\hat{q}_2}{1+\hat{x}}\frac{d\hat{q}_2}{d\hat{t}} - \frac{1}{2}\left[\frac{\hat{q}_2}{1+\hat{x}}\right]^2\hat{v} \end{cases}. \tag{35}$$

The energy balance for the electro-mechanical converter is then readily obtained as

$$\frac{d}{d\hat{t}}\left[\frac{1}{2}\frac{\hat{q}_1^2}{1-\hat{x}}+\frac{1}{2}\frac{\hat{q}_2^2}{1+\hat{x}}+\frac{\hat{\omega}_{el}}{\hat{\omega}_2}\frac{(\hat{q}_1+\hat{q}_2)^2}{2}-\hat{V}_{el}(\hat{q}_1+\hat{q}_2)+\frac{\hat{v}^2}{2\eta}+\frac{\hat{x}^2}{2\eta}\right] = -\frac{\hat{a}(\hat{t})\hat{v}}{\eta}-\frac{1}{\hat{\omega}_2}\left[\left(\frac{d\hat{q}_1}{d\hat{t}}\right)^2+\left(\frac{d\hat{q}_2}{d\hat{t}}\right)^2\right]-\frac{2\zeta}{\eta}\hat{v}^2. \tag{36}$$

Equation (36) states that the time derivative of the total energy of the system is equal to the mechanical input power minus the converted power, and minus the power dissipated by the viscous friction. Now, because in the asymptotic regime the total energy is a periodic function, the time-average of (36) over an oscillation period $\hat{T} = 2\pi/\hat{\omega}$ gives:

$$\hat{P}_{\text{out}} = \hat{P}_{\text{in}} - \hat{P}_{\text{loss}} \tag{37}$$

where $\hat{P}_{\text{in}}$ and $\hat{P}_{\text{loss}}$ are the mean mechanical extracted power and mean dissipated power, respectively

$$\begin{cases} \hat{P}_{\text{in}} = -\frac{1}{\hat{T}}\int_{\hat{t}}^{\hat{t}+\hat{T}}\frac{\hat{a}(\hat{t})\hat{v}}{\eta}d\hat{t} \\ \hat{P}_{\text{loss}} = \frac{1}{\hat{T}}\int_{\hat{t}}^{\hat{t}+\hat{T}}\frac{2\zeta}{\eta}\hat{v}^2 d\hat{t} \end{cases}. \tag{38}$$

Equation (37) simply expresses the fact that the mean converted power equals the mean input power minus the mean dissipated power.

ACKNOWLEDGMENT

The authors would like to thank Prof. G. Coppa, C. Borean, and F. Peinetti for useful discussions and TILAB for graduate fellowship support of F. Peano.

REFERENCES

[1] S. Roundy, P. K. Wright, and J. Rabaey, "A study of low level vibrations as a power source for wireless sensor nodes," *Comput. Commun.*, vol. 26, pp. 1131–1144, Jul. 2003.
[2] C. B. Williams and R. B. Yates, "Analysis of a micro-electric generator for microsystems," in *Proc. Transducers 95/Eurosensors IX*, 1995, pp. 369–372.
[3] R. Amirtharajah and A. P. Chandrakasan, "Self-powered signal processing using vibration-based power generation," *IEEE J. Solid-State Circuits*, vol. 33, pp. 687–695, 1998.
[4] N. N. H. Ching, H. Y. Wong, W. J. Li, P. H. W. Leong, and Z. Wen, "A laser-micromachined multi-modal resonating power transducer for wireless sensing systems," *Sens. Actuators A, Phys.*, vol. 97, pp. 685–690, Apr. 2002.
[5] P. Glynne-Jones, S. P. Beeby, E. P. James, and N. M. White, "The modeling of a piezoelectric vibration powered generator for microsystems," in *Proc. Transducers'01/Eurosensors XV*, vol. 1, Jun. 2001, pp. 46–49.
[6] N. S. Shenck and J. A. Paradiso, "Energy scavenging with shoe-mounted piezoelectrics," *IEEE Micro*, vol. 21, pp. 30–41, 2001.
[7] S. S. Lee and R. M. White, "Self-excited piezoelectric cantilever oscillators," in *Proc. Transducers 95/Eurosensors IX*, 1995, pp. 41–45.
[8] S. Meninger, J. O. Mur-Miranda, R. Amirtarajah, A. P. Chandrakasan, and J. H. Lang, "Vibration-to-electric energy conversion," *IEEE Trans. VLSI Syst.*, vol. 9-1, Feb. 2001.
[9] R. Amirtharajah, S. Meninger, J. O. Mur-Miranda, A. Chandrakasan, and J. Lang, "A micropower programmable DSP powered using a MEMS-based vibration-to-electric energy converter," in *Digest of Technical Papers IEEE International Solid State Circuits Conference*, Feb. 2000, pp. 362–363.
[10] T. Sterken, K. Baert, R. Puers, and S. Borghs, "Power extraction from ambient vibration," in *Proc. SeSens (Workshop on Semiconductor Sensors) 2002*, Nov. 2002, pp. 680–683.
[11] T. Sterken, K. Baert, R. Puers, S. Borghs, and R. Mertens, "A new power MEMS component with variable capacitance," in *Proc. 2003 Pan Pacific Symposium Conference*, Feb. 2003.
[12] G. M. Sessler, "Electrets," in *Topics in Applied Physics*. New York: Springer-Verlag, 1980, vol. 33.
[13] C. Thielemann and G. Hess, "A micromachined capacitive electret microphone," *SPIE*, vol. 3680, pp. 756–784, 1999.

Fabio Peano was born in Italy on December 3, 1977. He received the high school degree in 1996 and the Master degree in nuclear engineering from the *Politecnico di Torino*, Turin, Italy, on October 19, 2001 (master thesis: "Dynamics on nonneutral plasmas: interaction between vortices"). He has been working towards the Ph.D. degree in plasma physics at the *Politecnico di Torino*, Turin, Italy, since January 2002.

He attended a summer class on topology and applied math at the *Universidade Federal de Pernambuco*, Recife, Brazil, January through February 2002. He was teaching assistant of Calculus at the Politecnico di Torino, Turin, Italy, from October through December 2002 and September through November 2003. He worked as a part-time collaborator at Telecom Italia Lab, Turin, Italy, from October 2002 to October 2003 (research topic: feasibility analysis of micro power supplies for autonomous MEMS devices). From November 2003 to July 2004, he was a visiting Ph.D. student at the Instituto Superior Técnico (IST), Lisbon, Portugal (research topic: interaction of ultra-intense laser pulses with molecular clusters). His current research interests are nonlinear phenomena in plasma physics, and intense laser-plasma interactions as particle and radiation sources for applications to biology (e.g., proton therapy in cancer treatments).

Mr. Peano is a Member of the Istituto Nazionale di Fisica della Materia (INFM) and of the Gruppo Nazionale di Fisica Matematica (GNFM).

Tiziana Tambosso (M'94–SM'01) received the M.S. and Ph.D. degrees in optoelectronic engineering from University of Pavia, Italy, in 1983 and 1988, respectively.

She has been a researcher at University of Pavia giving contributions in optoelectronics (all-fiber passive components, fiber-optic sensors). From 1989 to 1993, she has been responsible for the fiber optic devices group at SIRTI, R&D Division, developing optical fiber couplers, attenuators and fiber optic amplifiers. In 1993 she joined CSELT (now TILAB), the Telecom Italia Group R&D laboratories, where, as head of a research group and project leader, she has been working on second window fiber-optic amplifiers, optical fibers, passive optical components, optoelectonics devices for millimeter waves generation, MEMS for e-tag powering and microsensors for e-tag ad-hoc networks. From 1993 to 1997, she has contributed to IEC standard activity as the Secretary of Subcommittee SC86B on fiber optic interconnecting devices and passive components. She has authored or coauthored about 50 papers in journals or conference proceedings, and holds nine patents.

Dr. Tambosso has promoted, as chairperson of the Technical Programme Committee, two editions of WFOPC, the International Workshop on Fibers & Optical Passive Components of IEEE-LEOS. She has served as Guest Editor of the IEEE Selected Topics in Quantum Electronics of Sept. 1999 on Fiber Optic Passive Components. She was engaged in the Technical Programme Committee of the OFC '01–'03 (Optical Fiber Communication Conference) and ECOC'03 (European Conference on Optical Communication). She is the Chairperson of the IEEE LEOS Italian Chapter.